BUCKLING OF BEAMS WITH A BOUNDARY ELEMENT TECHNIQUE

ABDERRAZEK MESSAOUDI[1*], LASZLO PETER KISS[1]

[1]*Institute of Applied Mechanics, University of Miskolc, 3515 Miskolc-Egyetemvaros, Hungary*

Abstract: The present work is devoted to the buckling study of non-homogeneous fixed-fixed beams with intermediate spring support. The stability issue of these beams leads to three-point boundary value problems. If the Green functions of these boundary value problems are known, the differential equations of the stability problems that contain the critical load sought can be turned into eigenvalue problems given by homogeneous Fredholm integral equations. The kernel function of these equations can be calculated from the associated Green functions. The eigenvalue issues can be reduced to algebraic eigenvalue problems, which are subsequently solvable numerically with the use of an efficient algorithm from the boundary element method. Within this article, the critical load findings of these beams are compared to those obtained using commercial finite element software, and the results are in excellent correlation.

Keywords: green function, fredholm integral equation, boundary value problem, buckling

1. INTRODUCTION

Buckling is a long-known phenomenon that can occur for various engineering structures [1, 2]. Since Euler's pioneering work, it is clear that buckling can as well happen to straight columns under compressive loads [3]. In the fields of mechanical, structural, and aeronautical engineering, buckling of beams subjected to compressive load is a prevalent problem. When a straight beam is loaded with an axially compressive force, minor deformations occur before reaching a critical load value that can initiate buckling. The calculation of the critical buckling load is important for compressed slender members that are in the focus of several researches, including static and dynamic, studies. Book [4], for example, is a thorough examination of the theory of elastic stability of continuously axially loaded columns, entirely focusing on column buckling. In study [5], the buckling instability of a system of three simply supported elastic Timoshenko beams linked by Winkler elastic layers with each beam subjected to the same compressive axial force is examined. In article [6], the elastic and geometric stiffness matrices are used for beams on an elastic foundation to find the buckling loads and mode shapes. A bunch of support conditions (rigid and elastic) are addressed in [7] when the stability of multi-step beams is investigated. The external loads can be composed of several forces. The transfer matrix method is used to find the solutions, which are compared with finite element findings. Laminated beams are in the spotlight in [8]. Since the model incorporates shearing, there are three independent kinematic unknown fields. The typical differential equations are found from a variational principle. The buckling loads are gained from the Ritz method by approximating the three fields with polynomials. A new numerical method is proposed in [9] for axially functionally graded beams. The related buckling differential equations with non-constant coefficients are replaced with linear algebraic equation systems to tackle the issue. It is also worthy to mention article [10] where the stability of imperfect stepped beams with cracks are studied. The applied method is the distributed line spring technique. Various stress concentration factors

[*] Corresponding author, email: abderrazek.messaoudi@uni-miskolc.hu https://doi.org/10.29081/jesr.v28i2.003

are as well investigated. In paper [11], authors deal with the issue of determining the critical load of beams with three supports when the intermediate support is also rigid. Using the boundary element method (BEM), they solved the eigenvalue issue that yields the critical loads using Green's function of the three-point boundary value problem. The first concept of the Green function was published by George Green in 1828. His book [12] presents, discusses, and demonstrates how to use the Green function approach to electrostatic issues governed by partial differential equations. In article [13], the Green function is explained in terms of three-point boundary value problems defined by linear ordinary differential equations. However, application is only given to vibrations.

The main goal of this research is to provide a novel solution to the stability problem of fixed-fixed beams with intermediate spring support (FssF, in short). Although the material is linearly elastic and isotropic, cross-sectional inhomogeneity can be handled as long as the material distribution varies throughout the cross-section only. The article applies the definition and the major properties of the Green function based on [11, 13] to construct it for the specified beam problem with two rigid and one elastic support. After that, it is possible to numerically solve the integral equation with the boundary element technique [14]. The results are evaluated graphically and are compared with finite element (FEM) findings. The correlation is very good.

2. MATERIALS AND METHODS

2.1. Governing equations

Figure 1 shows the considered heterogeneous FssF beam. The cross-sectional geometry of the beam is uniform throughout its length. The axis $\hat{x}$ of the coordinate system $\hat{x}\hat{y}\hat{z}$ corresponds with the *E*-weighted centerline of the beam. The symmetry plane in terms of geometry and material distribution of the beam is considered to be the coordinate plane $\hat{x}\hat{z}$. Thus, the modulus of elasticity *E* satisfies the relation $E(\hat{y},\hat{z}) = E(-\hat{y},\hat{z})$. The beam's length is *L*, and the location of the spring support is denoted by $\hat{b}$.

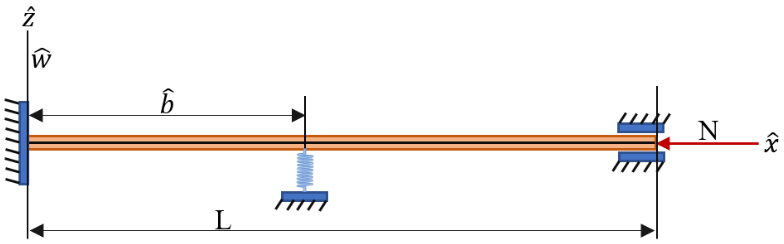

Fig. 1. A compressed fixed-fixed beam with intermediate spring support.

Along the beam centerline, we note that the *E*-weighted first moment $Q_{\hat{y}}$ is zero:

$$Q_{\hat{y}} = \int \hat{z}E(\hat{y},\hat{z})dA = 0 \tag{1}$$

when there is no axial load (*N=0*), the equilibrium problem of Euler-Bernoulli beams with cross-sectional heterogeneity is governed by the ordinary differential equation [15].

$$\frac{d^4\hat{w}}{d\hat{x}^4} = \frac{\hat{f}_z}{I_{ey}} \tag{2}$$

where $\hat{w}$ represents the vertical displacement of the material points of the beam centerline, $\hat{f}_z$ represents the intensity of the distributed load acting on the centerline, and I_{ey} is the flexural rigidity [15], defined by the equation:

$$I_{ey} = \int E(\hat{y},\hat{z})\hat{z}^2 dA \tag{3}$$

It is more convenient to introduce dimensionless variables as:

$$x = \frac{\hat{x}}{L} \quad , \quad \xi = \frac{\hat{\xi}}{L} \quad , \quad w = \frac{\hat{w}}{L} \quad , \tag{4a}$$

$$y = \frac{d\hat{w}}{d\hat{x}} = \frac{dw}{dx} \quad , \quad b = \frac{\hat{b}}{L} \quad . \; l = \frac{x}{L}\Big|_{X=L} = 1 \tag{4b}$$

With these notations, equation (2) becomes:

$$\frac{d^4 w}{dx^4} = f_z \quad , \quad f_z = L^3 \frac{\hat{f}_z}{I_{ey}} \tag{5}$$

This differential equation is paired with the boundary- and continuity conditions given in Table 1. So, the vertical displacements and rotations are zero at the ends, while the displacement, rotation, bending moment are continuous at *x=b*, but the shear force has a jump because of the elastic restraint.

Table 1. Boundary and continuity conditions.

Boundary conditions
$w(x=0)=0,\ w^{(1)}(x=0)=0\ ,\ w(x=l)=0,\ w^{(1)}(x=l)=0$
Continuity conditions
$w(x=b-0)=0, \quad w(x=b+0)=0$ $w^{(1)}(x=b-0)=w^{(1)}(x=b+0)\ , \quad w^{(2)}(x=b-0)=w^{(2)}(x=b+0)$ $w^{(3)}(x=b-0)-\chi w(x=b)=w^{(3)}(x=b+0)$

In the above table, the dimensionless spring stiffness was introduced as:

$$\chi = \frac{K}{I_{ey}} L^3 \tag{6}$$

where *K* is the rigidity of the linear spiral spring at the intermediate support. To find the dimensionless deflection *w,* this time, an integral equation approach is used. This unknown filed is sought by [12].

$$w(x) = \int_0^{\ell} G(x,\xi)\, f_z(\xi) d\xi. \tag{7}$$

Here *G* is the Green function. It is uniquely determined for the boundary value problem of differential equation (5) and the boundary and continuity conditions of Table 1.

2.2. Buckling problem formulation

The related differential equation for the heterogeneous beam without distributed load, but under a compressive axial force *N* is:

$$w^{(4)} = -\mathcal{N} w^{(2)}, \quad \mathcal{N} = \frac{L^2 N}{I_{ey}} \tag{8}$$

This, together with the conditions of Table 1, constitutes an eigenvalue problem for the unknown dimensionless buckling load $\mathcal{N}$, which in the eigenvalue. Substituting $-\mathcal{N}w^{(2)}$ for f_z in integral equation (7) returns:

$$w(x) = -\mathcal{N} \int_0^{\ell} G(x,\xi) \frac{d^2 w(\xi)}{d\xi^2} d\,\xi \tag{9}$$

Deriving it with respect to *x* and taking into account that the Green function should satisfy the boundary conditions, we get a homogeneous Fredholm integral equation [11]:

$$y(x) = \mathcal{N} \int_0^{\ell} K(x,\xi) y(\xi) d\xi, \qquad \frac{\partial^2 G(x,\xi)}{\partial x \partial \xi} = K(x,\xi) \tag{10}$$

So, the stability problem is now replaced by the integral equation (10). The kernel function is proportional to the Green function, so the next aim is to find it.

2.3. The kernel function

The Green function of the boundary value problem has the following structure [13]:

$$G(x,\xi) = \begin{cases} G_{1I}(x,\xi) & \text{if } x,\xi \in [0,b], \\ G_{2I}(x,\xi) & \text{if } x\in[b,l] \text{ and } \xi\in[0,b] , \\ G_{1II}(x,\xi) & \text{if } x\in[0,b] \text{ and } \xi\in[b,l] , \\ G_{2II}(x,\xi) & \text{if } x,\xi \in[b,l]. \end{cases} \tag{11}$$

These functions can be found in closed-form using the definition published in [11]. Accordingly, if $\xi\in [0, b]$, the typical functions are sought as:

$$\begin{aligned} G_{1I} &= \sum_{m=1}^{4}[a_{mI}(\xi) + b_{mI}(\xi)]w_m(x) \; ; \; x<\xi \\ G_{1I} &= \sum_{m=1}^{4}[a_{mI}(\xi) - b_{mI}(\xi)]w_m(x) \; ; \; x>\xi \\ G_{2I} &= \sum_{m=1}^{4} c_{mI}(\xi)w_m(x) \end{aligned} \tag{12}$$

here w_m is the general solution of the homogeneous equation $w^{(4)} =0$, that is, in details:

$$w = \sum_{m=1}^{4} a_m w_m = a_1+a_2x+a_3x^2+a_4x^3 \tag{13}$$

Thus, there are *12* unknowns. As per the definition, G_{1I} and its first two derivatives are continuous if $x=\xi$, while the third derivative with respect to *x* has a jump with magnitude *0.5*. The remaining *8* equations follow from the boundary and continuity conditions of Table 1. In this way determination of G_{1I}, G_{2I} require the solution of two inhomogeneous algebraic system of equations. Similarly, if $\xi= [b, \ell]$, the form of the Green function is:

$$\begin{aligned} G_{2II} &= \textstyle\sum_{m=1}^{4}[a_{mII}(\xi) + b_{mI}(\xi)]w_m(x); \; x<\xi \\ G_{2II} &= \textstyle\sum_{m=1}^{4}[a_{mII}(\xi) - b_{mI}(\xi)]w_m(x); \; x>\xi \\ G_{1II} &= \textstyle\sum_{m=1}^{4} c_{mII}(\xi)w_m(x) \end{aligned} \tag{14}$$

At this point, the coefficients b_{mI} are already known, so the *8* remaining coefficients can be found, again, from the boundary and continuity conditions. So, the Green function for the FssF beam is in hand at this stage. The kernel function has the following structure:

$$K(x,\xi) = \begin{cases} K_{1I}(x,\xi) & \text{if } x,\xi \in[0,b], \\ K_{2I}(x,\xi) & \text{if } x\in[b,l] \text{ and } \xi\in[0,b] , \\ K_{1II}(x,\xi) & \text{if } x\in[0,b] \text{ and } \xi\in[b,l] , \\ K_{2II}(x,\xi) & \text{if } x,\xi \in[b,l]. \end{cases} \tag{15}$$

where:

$$K_{1I}(x,\xi) = \frac{\partial^2 G_{1I}(x,\xi)}{\partial x \partial \xi} \quad , \quad K_{2I}(x,\xi) = \frac{\partial^2 G_{2I}(x,\xi)}{\partial x \partial \xi} \tag{16a}$$

$$K_{1II}(x,\xi) = \frac{\partial^2 G_{1II}(x,\xi)}{\partial x \partial \xi} \quad , \quad K_{2II}(x,\xi) = \frac{\partial^2 G_{2II}(x,\xi)}{\partial x \partial \xi} \qquad (16b)$$

Now the critical load can, for example, be calculated using the boundary element technique following the description of book [14].

3. RESULTS AND DISCUSSION

The numerical results are shown in Figure 2. Parameter *b* identifies the location of the middle spring support. It is enough to assess the interval *[0, 0.5]* because the end supports are identical. The other variable is $\sqrt{N_{crit}}/\pi$, that is proportional to the critical load. The beam acts as if it were a fixed-fixed beam when χ =0. If χ tends to infinity, the beam behaves as if it were a fixed-fixed beam with intermediate rigid roller support [11]. The typical curves are all nonlinear in the figure. The buckling load has a maximum at *b=0.5*, and this property is independent of the spring stiffness. On the other hand, greater spring stiffness means stiffer intermediate support, that makes the structure capable of bearing greater loads. Comparing the most distant results, i.e., when *b=0.5* and *K* is zero or tends to infinity, it can be concluded that the difference between the allowable load can increase by *86%* which indicates that the support stiffness really has an impact on the structural behavior.

The critical load values obtained from the boundary element approach are verified using finite element analysis with commercial software. Two models have been created; a *2D* model with homogeneous cross-section where the steel material is used and a *3D* model with heterogeneous cross-section, made up of *3* vertical layers as shown in Figure 3. The layers are perfectly bonded, and buckling was restrained to the plane $\hat{x}\hat{z}$. The typical data: $E_1 = 2e5$ N/mm^2 and $E_2=7e4$ N/mm^2 are the Young's moduli of the steel and aluminum material. It is simply assumed that $a=c= 10$ mm, $a_1= a_2=a/3$, the length L of the beam is *100* mm and the stiffness of the spring is $K=33\ 333$ N/mm. For all the simulations, the spring support has two degrees of freedom (translation along $\hat{z}$ axis and rotation about $\hat{y}$ axis.

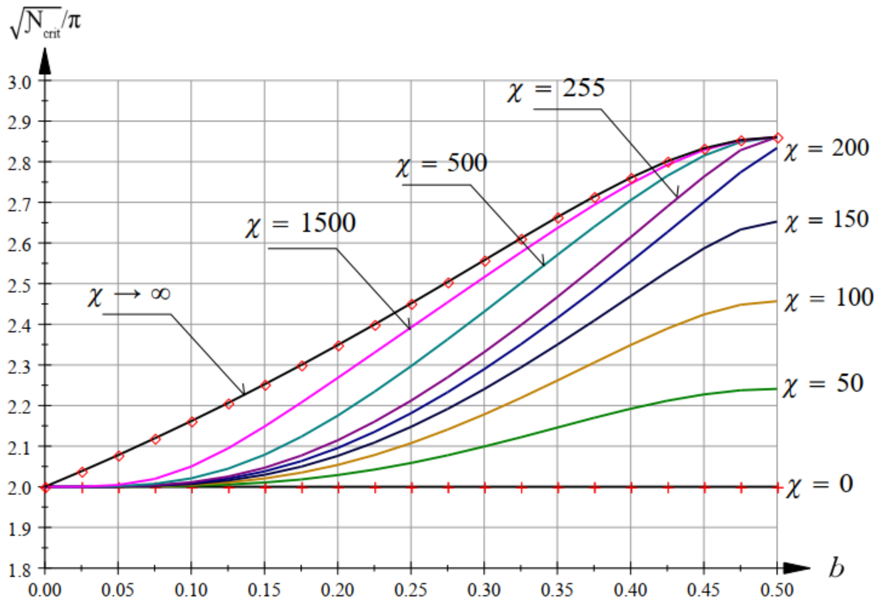

Fig. 2. Relationship between $\sqrt{N_{crit}}/\pi$ and spring support location.

If the beam is homogeneous steel,

$$I_{ey} = IE_1 = \frac{ac^3}{12} E_1 = \frac{10^4}{12} * 2 * 10^5 = 1.6667 * 10^8 \text{ N/mm}^2 \qquad (17)$$

$$\chi = \frac{K}{I_{ey}} L^3 = \frac{33333}{1.6667*10^8} * 100^3 = 200 \qquad (18)$$

If the beam is heterogeneous, then,

$$I_{ey} = \frac{ac^3}{12}\left[\frac{2*E_1+E_2}{3}\right] = \frac{10^4}{12}\left[\frac{2*2+0.7}{3}\right]10^5 = 1.3056*10^8 \text{ N/mm}^2 \quad (19)$$

$$\chi = \frac{K}{I_{ey}}L^3 = \frac{33333}{1.3056*10^8}*100^3 = 255 \quad (20)$$

According to Figure 2, when *b*= *0.5* we get $\sqrt{N_{crit,\ homo}}/\pi = 2.83379$ when χ=200 from where we have: $N_{crit,\ homo} = (2.83379*\pi)^2 = 79.25$ and $\sqrt{N_{crit,\ heter}}/\pi = 2.86060$ when $\chi = 255$ from where we have: $N_{crit,\ heter} = (2.86060*\pi)^2 = 80.76$. Substituting these to equation (8) yields:

$$N_{crit}(homogeneous) = \frac{I_{ey}\,N_{crit,homo}}{L^2} = \frac{1.6667*10^8*79.25}{100^2} = 13.208*10^5 \text{ N} \quad (21)$$

$$N_{crit}(heterogeneous) = \frac{I_{ey}\,N_{crit,heter}}{L^2} = \frac{1.3056*10^8*80.76}{100^2} = 10.544*10^5 \text{ N} \quad (22)$$

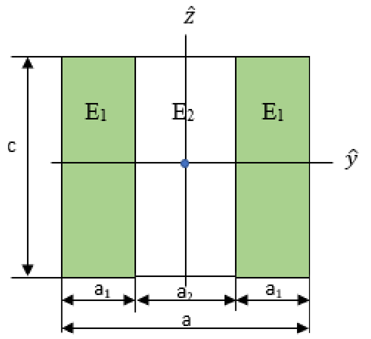

Fig. 3. The heterogeneous cross section of the selected beam.

Furthermore, Table 2 and 3 show the critical load findings for three intermediate support positions respectively using the boundary element method (BEM) and finite element method (FEM). In accordance with Figure 2, the results increase together with the middle support coordinate. The values are greater for homogeneous steel section, since it has a greater flexural rigidity. Furthermore, the one-dimensional BEM results are accurate enough. The maximum relative difference between the BEM and FEM models can be found when the cross-section is heterogeneous and *b=0.5*, this distinction is *3.2%* only.

Table 2. Critical loads results using the boundary element technique.

Spring support location (*b*)	Critical loads (*10^5*N)	
	Homogeneous FssF beams (χ=200)	Heterogeneous FssF beams (χ = 255)
0.00 or 1.00	6.57	5.14
0.25 or 0.75	7.81	6.29
0.5	13.20	10.54

Table 3. Critical loads results using the finite element method.

Spring support location (*b*)	Critical loads (*10^5*N)	
	2D homogenous FssF beams	3D heterogeneous FssF beams
0.00 or 1.00	6.60	5.04
0.25 or 0.75	7.67	6.00
0.50	12.82	10.36

The buckling mode shapes are normalized vectors and do not depict real deformation magnitudes at critical loads. They are normalized to a magnitude of 1.0 for the largest displacement component. Figure 4 shows the first buckling mode shape when b=0.25.

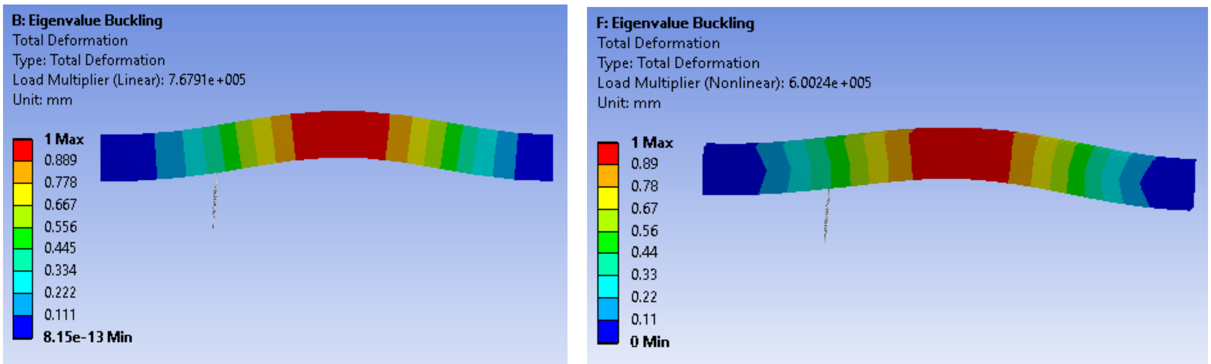

Fig. 4. First buckling mode shape (*b=0.25*): (a) *2D* model with homogeneous cross section; (b) *3D* model with heterogeneous cross section.

4. CONCLUSIONS

Within this article, the stability of compressed beams was investigated. The beams have uniform cross-section along the centerline, but the material distribution might be nonhomogeneous. Besides the classical end supports, there is an elastic third one in intermediate position. The validity of the Euler-Bernoulli hypothesis was assumed and the related ordinary differential equation was replaced by an integral equation during the proposed solution procedure. The critical loads are proportional to the eigenvalue while the kernel is the second derivative of the Green function in this formulation. Recalling the definition and the properties of the Green function for such boundary value problems, its construction was possible with the boundary and continuity conditions. With the Green function, it was possible to numerically solve the homogeneous Fredholm integral equation with boundary element technique. The results show the significant effects of the material composition, middle support position and spring stiffness on the lowest critical loads. When the spring stiffness of the middle support was zero, the structural element behaved as if it were only supported at the ends and if the stiffness was approaching to infinity, the intermediate support acted as a rigid roller. The numerical findings were compared with finite element computations and the correlation was found to be very good.

REFERENCES

[1] Baksa, A., Gonczi, D., Kiss, L.P., Kovacs, Z.P., Lukacs, Z., Experimental and numerical investigations on the stability of cylindrical shells, Journal of Engineering Studies and Research, vol. 26, no. 4, 2020, p. 34-39.
[2] Gonczi, D., Finite element investigation in the forming process of aluminium aerosol cans, Acta Technica Corviniensis – Bulletin of Engineering, vol. 13, no. 4, 2020, p. 19-22.
[3] Euler, K., Sur la force des colonnes, Memoires de V Academie de Barlin, Euler Archive at Scholarly Commons, 1759.
[4] Murawski, K., Technical stability of continuously loaded thin-walled slender columns, Lulu Press, 2017.
[5] Stojanovic, V., Kozic, P., Janevski, G., Buckling instabilities of elastically connected Timoshenko beams on an elastic layer subjected to axial forces, Journal of Mechanics of Materials and Structures, vol. 7, no. 4, 2012, p. 363–374.
[6] Eisenberger, M., Yankelevsky, D.Z., Clastornik, J., Stability of beams on elastic foundation, Computers and Structures, vol. 24, no. 1, 1986, p. 135–139.
[7] Li, Q.S., Buckling of multi-step non-uniform beams with elastically restrained boundary conditions, Journal of Constructional Steel Research, vol. 57, no. 7, 2001, p. 753–777.
[8] Aydogdu, M., Buckling analysis of cross-ply laminated beams with general boundary conditions by Ritz method, Composites Science and Technology, vol. 66, no. 10, 2006, p. 1248–1255.
[9] Huang, Y., Luo, Q.Z., A simple method to determine the critical buckling loads for axially inhomogeneous beams with elastic restraint, Computers and Mathematics with Applications, vol. 61, no. 9, 2011, p. 2510–2517.
[10] Lellep, J., Kraav, T., Buckling of beams and columns with defects, International Journal of Structural Stability and Dynamics, vol. 16, no. 8, 2016, article no: 1550048.
[11] Kiss, L., P., Szeidl, G., Abderrazek, M., Stability of heterogeneous beams with three supports through Green functions, Meccanica, vol. 57, no. 6, 2022, p. 1369-1390.

[12] Green, G., An essay on the application of mathematical analysis to the theories of electricity and magnetism, Notthingam, 1828.
[13] Szeidl, G., Kiss, L.P., Green functions for three point boundary value problems with applications to beams. advances in mathematics research, New York: Nova Science Publisher, 2020, p. 121–161.
[14] Szeidl, G., Kiss, L.P., Mechanical vibrations - an introduction, foundation of engineering mechanics, Springer Nature, Switzerland, 2020.
[15] Baksa, A., Ecsedi, I., A note on the pure bending of inhomogeneous prismatic bars, International Journal of Mechanical Engineering Education, vol. 37, no. 2, 2009, p. 108–129.